

Development of Nanocarbon Black-enabled Self-strain Sensing Ultra-high-performance Cementitious Composites

ABASAL HUSSAIN, TAO YU and FANGXIN ZOU

ABSTRACT

In this study, nanocarbon black (nCB) is employed to make the matrix of UHPC conductive. The nCB-UHPC composite is investigated for its fresh and hardened mechanical properties, piezoresistive behavior and microstructure. Piezoresistive behavior and strain sensitivity are measured by fractional change in electrical resistivity (FCR) with applied stress/strain. The nCB-UHPC composite exhibits adequately good workability (slump spread ≥ 170 mm), compressive strength of more than 144 MPa and an outstanding sensitivity (gauge factor > 130) achieved with 1.5% nCB. Additionally, it has shown a repeatable, highly sensitive compressive strain response up to 40 MPa. The proposed high-sensitivity nCB-UHPC composite demonstrates significant potential in becoming a field-deployable solution for the health monitoring of concrete infrastructure.

INTRODUCTION

Rapid advancement in concrete technology has been observed in the past three to four decades. Ultra-high-performance concrete (UHPC) and smart concrete (self-healing, self-sensing, self-compacting) are the most desired achievements in concrete technology. Developing new functionalities in cementitious-based materials can change the concept from strength-only performance to multifunctionality in the construction industry, which is enabled by adding different versatile and innovative materials [1]. However, durability problems are still under consideration for the long-term serviceability of concrete structures.

For long-term performance monitoring of concrete infrastructure, different electronic sensors are used to sense strain, damage, temperature, humidity, and other parameters [2, 3]. Although these sensors generally perform better, their incompatibility with concrete structures, short lifetime, skilled labor demand and high cost for installation and maintenance limits their large-scale application in civil infrastructure [4]. Cementitious smart sensor is the new concept in the construction industry to replace

Abasal Hussain, Department of Civil and Environmental Engineering, The Hong Kong Polytechnic University, Hung Hom, Kowloon, Hong Kong SAR, China

Tao YU, Department of Civil and Environmental Engineering, The Hong Kong Polytechnic University, Hung Hom, Kowloon, Hong Kong SAR, China

Fangxin ZOU, Department of Aeronautical and Aviation Engineering, The Hong Kong Polytechnic University, Hung Hom, Kowloon, Hong Kong SAR, China

traditional electronic sensors. These sensors are fabricated by the addition of different micro and nano-level conductive materials like carbon black [5], carbon fiber [6], carbon nanotubes [7], steel fiber [8-10] and other hybrid [11] materials into the cementitious matrix. Therefore, it can be used as a structural material that can intrinsically sense its stress/strain, crack, and damage.

Many researchers have investigated cementitious sensors by employing normal cement paste, mortar, and concrete with various conductive materials. Only a few investigations have been conducted using UHPC with carbon nanotubes (CNT) and steel fiber to sense the crack and compressive strain. S.H. Lee et al. [12] used steel fiber and CNT to produce the self-sensing UHPC. The compressive piezoresistive behavior of UHPC with steel fiber and CNT cannot be monitored. It is attributed that the mobility of the CNT and steel fiber is very limited in compression because of the dense microstructure of the UHPC.

Lee et al. [13] incorporated the aggregate of fine steel slag to replace the normal sand with steel fiber into the UHPC matrix to investigate the piezoresistive behavior. The self-strain sensing ability under compression is achieved instead of a highly dense microstructure. It is attributed to the matrix's conductive phase by adding steel slag, which helps to enhance sensitivity. It has been noticed that matrix conductivity is a critical factor for the sensing behavior of the sensor. Thus, the conductive matrix will be beneficial to enhance piezoresistive behavior. At the same time, the studies utilize CNT as a conductive phase material. It has significant dispersion issues and a high cost, which precludes its use in concrete structures. Compared to nanofillers, nanocarbon black is one of the most promising candidates for producing cementitious sensors because of its permanent electric conductivity, low cost, better thermal and chemical stability, reproducibility, repeatability, and filler effect to improve the mechanical properties of conductive concrete.

Therefore, this study considers all the above parameters; conductive high-structure nanocarbon black (nCB) is regarded as a conductive material incorporated in ultra-high-performance concrete. To the best of our knowledge, this is the first work to demonstrate the compressive piezoresistive behavior of UHPC using cost-effective nanocarbon black by using the conductive matrix approach, which will help to demonstrate the piezoresistive behavior to an applied load. As a result, this new multifunctional UHPC composite material can be used in civil infrastructure to enhance the serviceability and real-time monitoring of structural health, which will help to significantly reduce unexpected accidents, saving human life and resources, as well as the maintenance cost in the later stages.

EXPERIMENTAL PROGRAM

Raw Materials and Mixed Design

This study uses ordinary Portland cement (OPC CEM I 52.5N), silica fume and quartz powder. The river sand with a particle size larger than 1.18 mm was sieved by the recommendation of the authors [14] is used. A polycarboxylate-based superplasticizer was used. The solid content of the superplasticizer was 22% by mass and a specific gravity of 1.05. Nanocarbon black with oil absorption number (OAN) 290 ml/100gm is used as a conductive material. The density of nCB is 0.16 g/cm³, resistivity 0.18 ohm-cm, and the particle size 40 nm, respectively.

TABLE I. BASE MIX DESIGN OF UHPC-NCB

Notation	Cement	Silica fume	Quartz powder	Sand	Water	SP	nCB
UHPC-nCB	1.0	0.25	0.25	1.10	0.19	0.05	0.0 - 0.02

In this study, nCB is used as a piezoresistive material to improve the electromechanical properties of the UHPC. The UHPC utilizes a low water-to-cement content, which is around 0.2. Even though producing a good UHPC is challenging with that low water-to-cement ratio, the addition of nanofiller makes it more problematic by absorbing much water. The final mixed design is detailed in Table I.

Specimen Preparation and Fresh Properties

Two main and four sub-steps are employed for manufacturing UHPC-nCB composite. The first major step is to manufacture of UHPC matrix, and the second major step is the addition of nCB and casting of sensors. It can be explained in the step-by-step preparation of the UHPC-nCB specimen. The first step is to mix dry ingredients (i.e., cement, quartz powder, silica fume and sand) for five min; then add 75-85% of water with a superplasticizer to the mixture in two stages and continue mixing until a slurry of UHPC is ready. After that, nCB is added with the remaining SP and water and continues the mixing until the UHPC reaches an acceptable fluidity level.

The flowability of the fresh mixed UHPC matrix is tested according to C1437/C1437M-15 [15]. The UHPC-nCB mix was poured into oiled molds.

Mechanical Testing

According to ASTM C109 [16], the 50 mm cubic samples were prepared for the compressive test and the copper mesh was embedded for piezoresistive testing. After the casting, the samples were covered with a plastic sheet within 10 minutes and left for 24 hours at room temperature. After demolding, the specimens were put in normal tap water for 28 days at $22^{\circ}\text{C} \pm 3^{\circ}\text{C}$. For each curing system, three specimens were tested to obtain an average value. The loading rate is 1MPs/s applied for the compression test.

Piezoresistive Properties

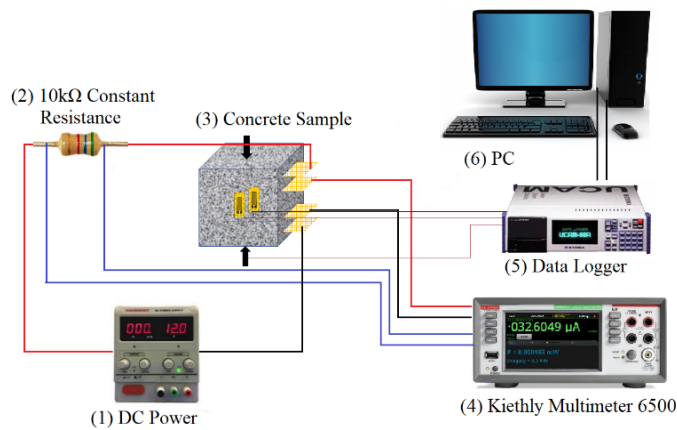


Figure 1. Schematic diagram to measure the piezoresistive behavior of UHPC-nCB sensors.

A four-probe testing method is employed for the resistance measurement to avoid contact resistance. The two-probe method added a contact resistance to the actual specimen resistance, not the real resistance of the specimen [17]. Four copper mesh lengths of 50 mm and 10 mm width were embedded during the sample preparation to perform the piezoresistive test of the UHPC sensors. The distances between the inner electrodes are 20 mm, and the cover and outer electrodes are 7.5 mm apart. Before undergoing the cyclic compressive test, the samples were dried out at 80 °C for 72 hours to reduce the moisture content.

The measurement of piezoresistive behavior during the compressive cyclic loading and monotonic loading was performed. The sample is loaded by displacement control with a 0.4mm/min loading rate and four cycles of repeated compressive loading. The axial strain was measured by the strain gauges attached to two opposite sides of the sample. The data logger recorded the strain data. The outer two electrodes are engaged to apply the direct current throughout the cyclic compressive loading, and the inner electrodes are used to determine the voltage by a digital multimeter Keithley DMM6500. The detailed circuit is plotted in Fig 1.

The given equation calculates the fractional change in resistance.

$$FCR = \frac{R - R_0}{R_0} \times 100\% \quad (1)$$

where FCR is the fractional change in resistance, R shows the initial resistance before applying load, and R₀ is the resistance during cyclic loading.

RESULT AND DISCUSSIONS

Flowability of nCB-Filled Composites

The flowability of the fresh mixed UHPC with the addition of nCB is comprehensively investigated to meet the fresh and hardened properties of nCB-incorporated UHPC.

TABLE II. COMPRESSIVE STRENGTH AND FLOWABILITY PROPERTIES

Notation	Compressive Strength (MPa)		Flowability (mm)
	Mean	SD	
PC	183.9	6.83	331
nCB0.25	168.5	3.95	282
nCB0.50	158.7	1.57	240
nCB0.75	151.7	2.37	218
nCB1.00	150.4	0.91	193
nCB1.25	147.5	3.73	181
nCB1.50	144.8	3.72	170
nCB1.75	142.5	3.07	158
nCB2.00	141.6	3.51	143

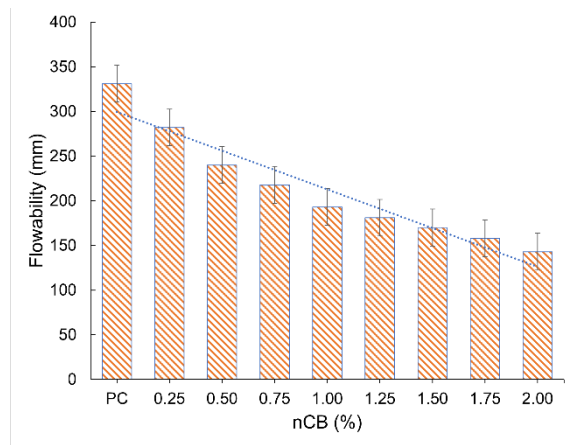


Figure 2. Flowability of the UHPC with nanocarbon black content.

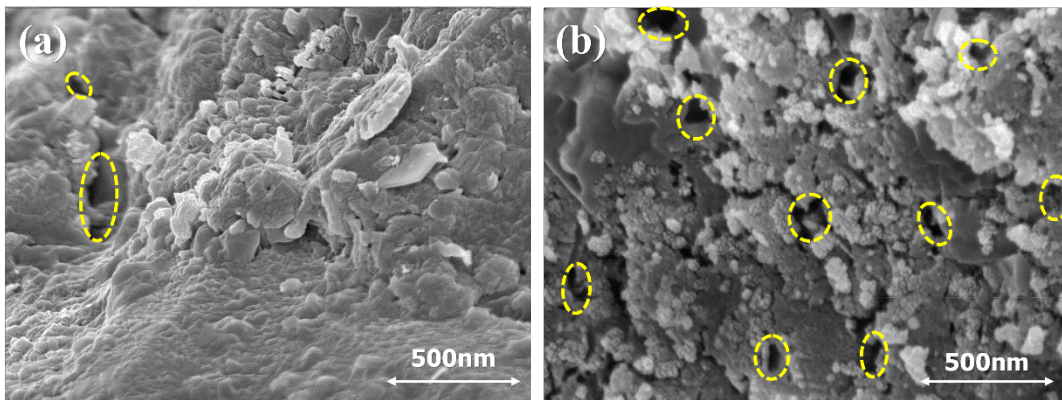


Figure 3. Microstructure of UHPC-nCB composites (a) 0.5% nCB and (b) 2.0% nCB.

There are eight groups of UHPC with different nCB content, and a plain UHPC investigated the mechanical and piezoresistive behavior. The flowability of the mixes was measured by the flow table apparatus on horizontal and vertical sides and took the mean. From Table II, the flowability of the mix design is gradually decreased with the increasing content of nCB. Plain concrete has the highest flowability, which is 331mm. It can be observed from Fig. 2 that with the addition of the nCB, the flowability is steadily reduced to 143 mm with 2.0% nCB. The decreasing flowability with the increasing content of nCB is due to water absorption of the nCB, which increases the viscosity of the matrix. Flowability with 2.0% nCB is reduced by 57% compared to plain UHPC. However, at the flowability of 1.50%, nCB has the better flowability, which is the percolation zone (0.50 % - 1.50 %) for piezoresistive behavior.

Compressive Strength

The compressive strength test results can be seen in Table II. The 28 days of water immersion compressive strength results in a decrease as the nCB content is increased. The flowability results are directly related to compressive strength, which can be evidence of the flowability reduction. The minimum compressive strength is 141.6MPa with 2.0% nCB at 28 days which is a 22.9% reduction in compressive strength. However, it is still higher than the code requirement. It can also be seen from Fig. 3 that

the nCB particles have an agglomeration, create stress concentration points, and increase porosity. When the nanoparticles of carbon black are added to a concrete mix, they absorb an excessive amount of water, which reduces the flowability of the fresh concrete. As the nCB increases, the flowability further decreases, which causes improper matrix compaction and a higher number of voids, and as a result, the compressive strength of the mix is reduced.

Piezoresistive Behavior

The piezoresistive behavior during repeated cyclic loading can be seen in Fig. 4 (a). It can be said that the results presented have a clear synchronization of the fractional change in resistance (FCR) with uniaxial cyclic compressive strain. When the load is applied, the resistance of the sensor is decreased, and it increases as the unloading. It can be attributed that the distance between the nanocarbon black particles is decreased when the load is applied, which reduces the particle-to-particle distance and reconstruction of the new conductive pathways by quantum tunneling phenomena during the compressive loading. Likewise, the distance between nanoparticles increases and the interruption of the conductive paths occurs during the unloading, so the resistance increases again.

The 1.50% nCB, the upper limit of the percolation threshold, has shown the highest FCR corresponding to strain. After that, the FCR starts to decrease in the above percolation zone. At the above percolation zone, the conductive path is already formed as particles are closely packed and, in some cases, in-state of overlap. The strain sensitivity of the samples is evaluated by using a linear fitting curve. The slope of the fractional change of electrical resistance with respect to the applied strain considers a gauge factor of strain sensors [18].

The strain sensitivity, measured by the gauge factor (GF) of all the samples, is evaluated by Equation 3.

$$GF = \frac{FCR}{\Delta \varepsilon} \quad (2)$$

FCR is the fractional change in resistivity and $\Delta \varepsilon$ is the change in compressive strain.

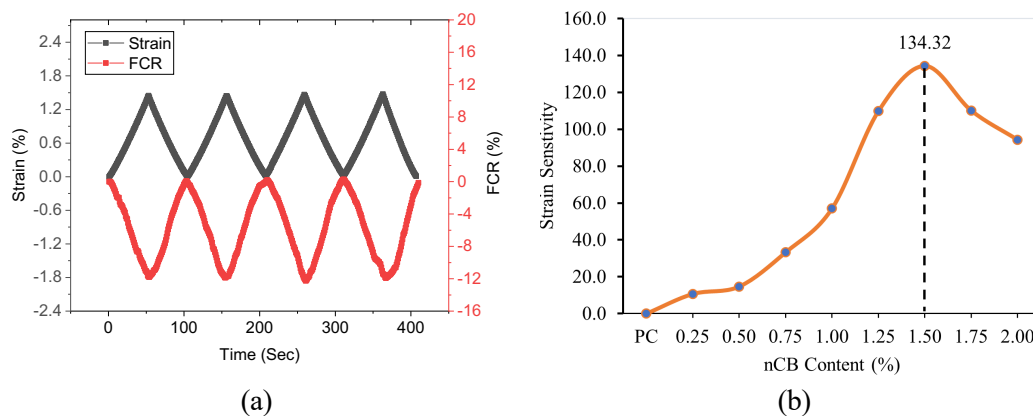


Figure 4. The piezoresistive behavior of the 1.50% nCB: (a) cyclic FCR to applied strain and (b) strain sensitivity.

The gauge factor is obtained from a simple linear regression slope employed to evaluate the gauge factor of the samples. From Fig. 4(b), it can be observed that the nCB with 1.50% content has shown the highest gauge factor, 134.32. As observed from the previous cyclic compression results, the 1.5% nCB has the highest FCR in cyclic loading. It can be observed from the percolation threshold graph that the 0.50-1.50% nCB is at the percolation zone. Carbon black with 0.50% is the starting point of the percolation zone. As the nanocarbon black content increases, the relationship between fractional change in electrical resistance and strain is more linear and improved.

CONCLUSION

To date, this is the first study to explore the strain-sensing capabilities of ultra-high-performance concrete (UHPC) using chain-structured, cost-effective nanocarbon black (nCB). The flowability (>170 mm) and the compression strength (>144 MPa) of UHPC-nCB with 1.50% have shown reasonable results. A low percolation zone (0.50-1.50%) has been achieved with a precise repeatable and synchronized FCR response up to a stress amplitude of 40 MPa and strain sensitivity (gauge factor > 134).

REFERENCES

1. Soliman, N.A., *Electric energy dissipation and electric tortuosity in electron conductive cement-based materials*. 2020.
2. Taheri, S., *A review on five key sensors for monitoring of concrete structures*. Construction and Building Materials, 2019. **204**: p. 492-509.
3. Sikarwar, S. and B.C. Yadav, *Opto-electronic humidity sensor: A review*. Sensors and Actuators a-Physical, 2015. **233**: p. 54-70.
4. Ou, J.P., *Research and practice of intelligent sensing technologies in civil structural health monitoring in the mainland of China - art. no. 61761D*. Nondestructive Evaluation and Health Monitoring of Aerospace Materials, Composites, and Civil Infrastructure V, 2006. **6176**: p. D1761-D1761.
5. Monteiro, A.O., et al., *A pressure-sensitive carbon black cement composite for traffic monitoring*. Construction and Building Materials, 2017. **154**: p. 1079-1086.
6. Azhari, F. and N. Bantia, *Cement-based sensors with carbon fibers and carbon nanotubes for piezoresistive sensing*. Cement & Concrete Composites, 2012. **34**(7): p. 866-873.
7. Naqi, A., et al., *Effect of multi-walled carbon nanotubes (MWCNTs) on the strength development of cementitious materials*. Journal of Materials Research and Technology, 2019. **8**(1): p. 1203-1211.
8. Hussain, A., et al., *Study on self-monitoring of multiple cracked concrete beams with multiphase conductive materials subjected to bending*. Smart Materials and Structures, 2019. **28**(9): p. 95003-95003.
9. Ding, Y., et al., *Effect of steel fiber and carbon black on the self-sensing ability of concrete cracks under bending*. Construction and Building Materials, 2019. **207**: p. 630-639.
10. Hussain, Z., et al., *Effect of fiber dosage on water permeability using a newly designed apparatus and crack monitoring of steel fiber-reinforced concrete under direct tensile loading*. Structural Health Monitoring, 2021: p. 147592172111052855.
11. Ahmed, S., et al., *Effect of Carbon Black and Hybrid Steel-Polypropylene Fiber on the Mechanical and Self-Sensing Characteristics of Concrete Considering Different Coarse Aggregates' Sizes*. Materials, 2021. **14**(23): p. 7455.
12. Lee, S.H., S. Kim, and D.Y. Yoo, *Hybrid effects of steel fiber and carbon nanotube on self-sensing capability of ultra-high-performance concrete*. Construction and Building Materials, 2018. **185**: p. 530-544.
13. Lee, S.Y., H.V. Le, and D.J. Kim, *Self-stress sensing smart concrete containing fine steel slag aggregates and steel fibers under high compressive stress*. Construction and Building Materials, 2019. **220**: p. 149-160.

14. Wille, K. and C. Boisvert-Cotulio, *Material efficiency in the design of ultra-high performance concrete*. Construction and Building Materials, 2015. **86**: p. 33-43.
15. Astm, *Standard Test Method for Flow of Hydraulic Cement Mortar: C1437-01*. Standard, 2001: p. 7-8.
16. International, A., *C109/C109M-05. Standard Test Method for Compressive Strength of Hydraulic Cement Mortars*. Annual Book of ASTM Standards, 2005. **04**: p. 9-9.
17. Chung, D.D.L., *A critical review of piezoresistivity and its application in electrical-resistance-based strain sensing*. Journal of Materials Science, 2020. **55**(32): p. 15367-15396.
18. Amjadi, M., et al., *Stretchable, Skin-Mountable, and Wearable Strain Sensors and Their Potential Applications: A Review*. Advanced Functional Materials, 2016. **26**(11): p. 1678-1698.